Single Frequency 2-D Leaky-Wave Beam Steering Using an Array of Surface-Wave Launchers

Symon K. Podilchak [1,2], Al P. Freundorfer [2], Yahia M. M. Antar [1,2]

[1]*Department of Electrical and Computer Engineering, Royal Military College of Canada*
Kingston, ON, Canada (antar-y@rmc.ca)
[2]*Department of Electrical and Computer Engineering, Queen's University*
Kingston, ON, Canada

***Abstract*— A planar antenna that utilizes surface-waves (SWs) for leaky-wave (LW) excitation is presented for millimeter-wave applications. Specifically, a two element array of directive Yagi-Uda like surface-wave launchers (SWLs) is used as the antenna feed, exciting cylindrical SWs on a grounded dielectric slab. By varying the relative phase difference between elements, the excited SW field distribution can be controlled. With the addition of metallic circular strip gratings, suitable conditions for LW excitation can be achieved. Essentially cylindrical LWs can be steered to confined regions on the guiding surface. For instance, by changing the relative phase difference between SWL sources such aperture fields can produce pencil and conical-sector beam patterns that can be steered in the far field at a single frequency. To the authors knowledge this is the first time such a LWA has been designed, fabricated and measured.**

I. Introduction

High gain leaky-wave antennas (LWAs) have been utilized in the design of many radar and satellite communication systems. In particular, planar 2-D LWAs are advantageous for their compatibility with monolithic devices, low cost and directive beam patterns. These antennas are characterized by a suitable aperture and source configuration and far field beam scanning is inherently observed as a function of frequency [1].

Recently, single source surface-wave launchers (SWLs) have been shown to be a practical feeding technique [2], [3] for such planar 2-D LWAs [4], [5]. Essentially, slotted configurations in the ground plane can couple energy into the dominant TM_0 surface-wave (SW) mode of the slab. With the addition of appropriately designed gratings or strips, leaky-waves (LWs) can be excited, realizing the transformation from a bound mode to a radiated mode.

A two element linear array of such SWLs [6] has also been used to steer the SW field distribution on a grounded dielectric slab (GDS). Essentially, SWs can be steered at a single frequency by varying the relative phase difference ($\delta = \Phi_2 - \Phi_1$) between SWL elements. In this work a continuous circular grating configuration is investigated as shown in Fig. 1. Thus, by using such a symmetric SWL array, LW field excitation on the guiding surface can be tuned offering 2-D beam steering in the far field. To the authors knowledge this is the first time such a circular grating LWA has been designed, fabricated and measured realizing the control of LW field distributions on a guiding surface at a single frequency.

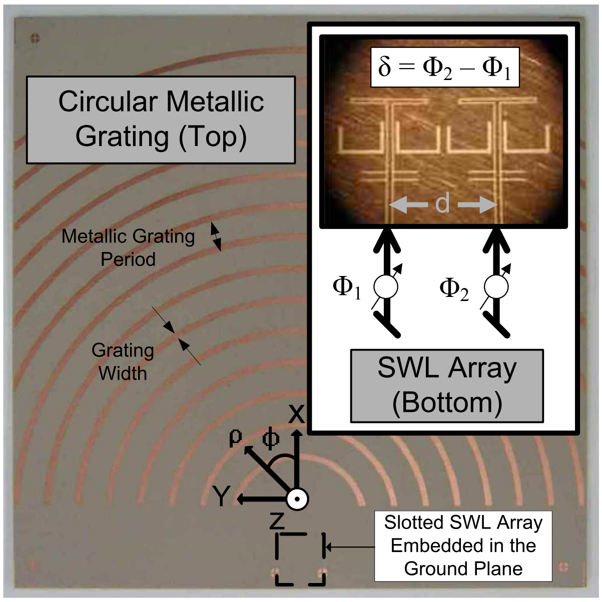

Fig. 1. By variation in δ the two element array of SWLs can excite cylindrical SWs that can be steered. Using a continuous circular strip grating, LWs can be excited and thus directive beam patterns can be controlled in the far field.

II. Individual Surface-Wave Launcher Operation and Arrayed Configuration for Beam Steering

The coplanar waveguide (CPW) transmission line (TL) fed SWLs were realized by slots in the ground plane of a GDS. Essentially, the slotted configurations act as magnetic dipole sources for the investigated planar LWA and cylindrical SWs are excited on the guiding surface. Unidirectional SW propagation is achieved by the addition of secondary reflector slots [2]-[6]. In addition, substrate properties ($\epsilon_r = 10.2$, $h = 1.27$ mm and $\tan\delta = 0.0023$) were properly chosen such that approximately 85% of the input power was coupled into the dominant TM_0 SW mode of the slab [2].

A. Folded Secondary Slot Surface-Wave Launchers

In general, reflector-based SWLs have secondary slots that are slightly longer than the main slot [2], [3]. For the desired

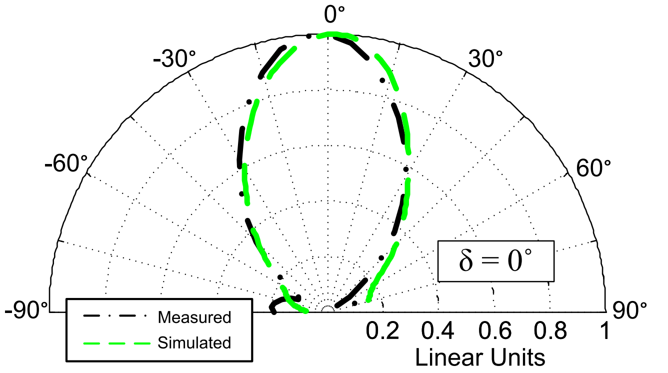

Fig. 2. Field distribution on top of the slab (with no gratings) generated by the array of SWLs for $\delta = 0°$. By changing the relative phase difference between SWL elements the total SW beam pattern can be controlled.

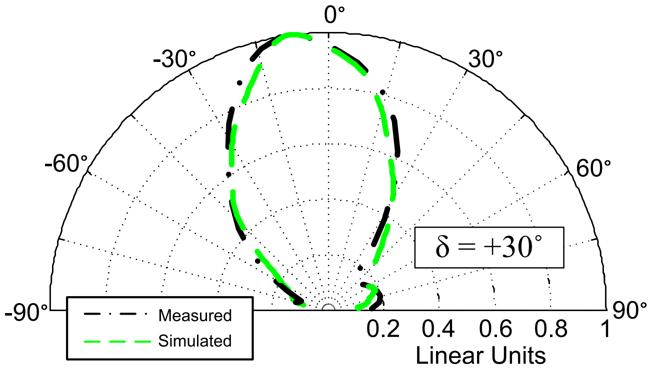

Fig. 3. Controlled SW field distribution on top of the slab for $\delta = +30°$ (no gratings). It can be observed [expected] that for $\delta = +[-]30°$ the main SW beam is steered $-[+]8°$ with side lobes $75°$ away from the main beam.

arrayed configuration of two SWL sources (separated by a distance of $d = \frac{\lambda^{SW}}{2}$) the secondary reflector slots were folded. Without such folding the SWLs would physically touch. This is unwanted since minimum mutual coupling is required between the SWLs for efficient operation [6].

B. Steered Surface-Wave Beam Patterns

The measured SW field distributions generated by the symmetric SWL array are shown in Figs. 2-5 and values are compared to the simulated results for relative phase differences of $\delta = 0°, +30°, +60°$ and $+90°$. Similar values are expected for a negated phase difference. The steered SW field distributions were measured using a near field probe (0.5 mm above the air-dielectric interface) on an arc centered (radius, $r_0 = 4.5$ cm and $r_0 >> \lambda^{SW}$) at the SWL elements. No gratings or strips were included in the measurement. The SWL array was placed at the edge of the high permittivity substrate and relative phase values were tuned by adjusting the phase of the SWLs using a mechanical phase shifter (see Fig. 6).

The evanescent fields along this arc represent the SW field distributions at a significant distance away from the SWLs and thus can represent the SW beam pattern on the GDS [6].

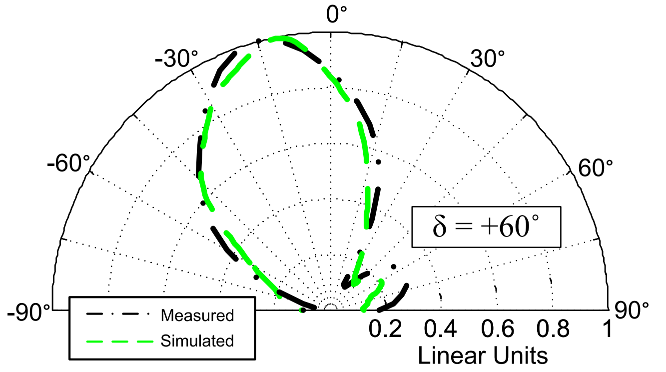

Fig. 4. Controlled SW field distribution on top of the slab for $\delta = +60°$ (no gratings). It can be observed [expected] that for $\delta = +[-]60°$ the main SW beam is steered $-[+]12.5°$ with side lobes $87°$ away from the main beam.

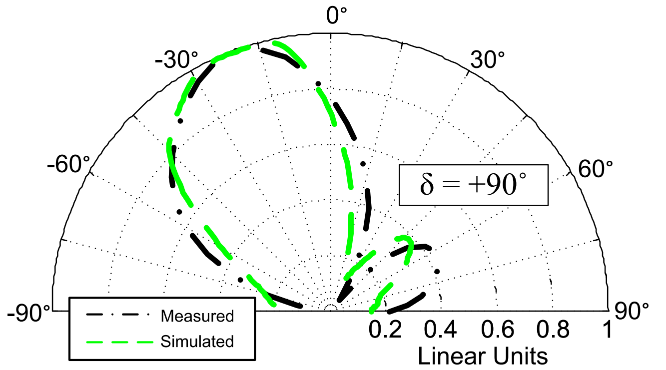

Fig. 5. Controlled SW field distribution on top of the slab for $\delta = +90°$ (no gratings). It can be observed [expected] that for $\delta = +[-]90°$ the main SW beam is steered $-[+]18°$ with side lobes $102°$ away from the main beam.

In addition, measurements were aperture gated (to eliminate multiple reflections from the edges of the guiding structure and unwanted image sources) and time gated (to reduce high frequency noise, multiple reflections due to cable bending and field probe discontinuities from VNA measurements).

III. A Circular Strip Grating Leaky-Wave Antenna Offering Conical-Sector Beam Steering

If a metallic grating is placed a suitable distance from the two element SWL array (and on top of the GDS) LWs can be excited. The printed metallic grating defines an effective partially reflective surface and LW radiation is achieved by a fast $n = -1$ spatial harmonic. Circular gratings are optimal since the periodic metallic strips are conformal to the cylindrical phase front generated by the SWLs [5]. Essentially, suitable boundary conditions are appropriate for TM_z cylindrical LW excitation on the guiding surface [1]. Since the steered SW fields from the SWL array are directed on the GDS, the cylindrical LWs are contained within a specified region as well. Essentially, the steered SW field distribution dictates the region of LW field excitation on the guiding surface, realizing controlled conical-sector beam steering in the far field.

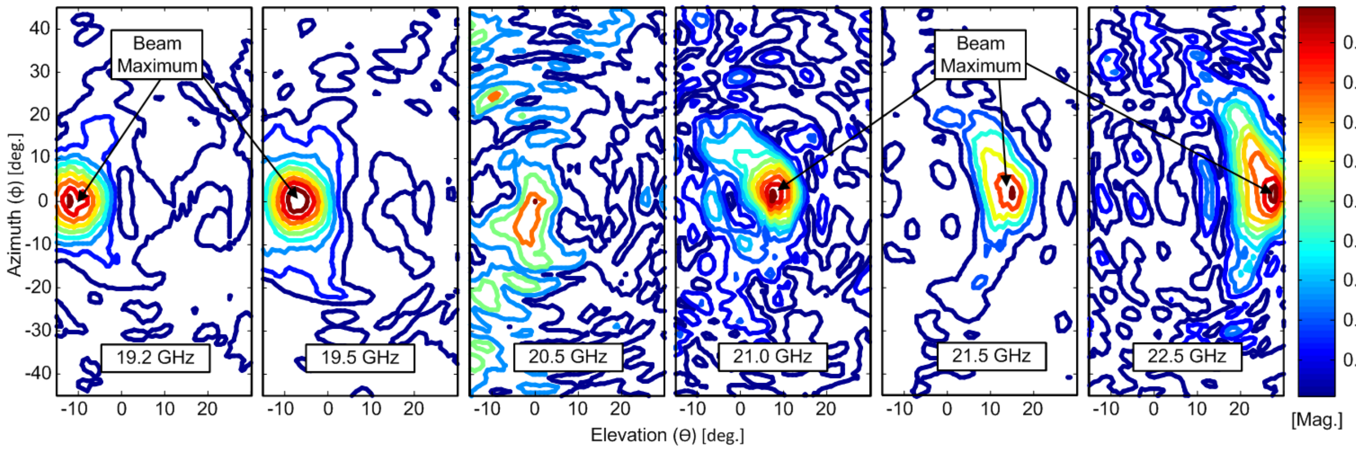

Fig. 7. Measured far field beam patterns at 19.2, 19.5, 20.5, 21.0, 21.5 and 22.5 GHz for $\delta = 0°$ (normalized to maximum gain observed at 21.5 GHz and shown in linear units). A confined pencil beam [LW stopband] $\langle$scanned conical-sector beam$\rangle$ is observed for $f \le 21$ [$f = 20.5$] $\langle 21 \le f \le 23 \rangle$ GHz.

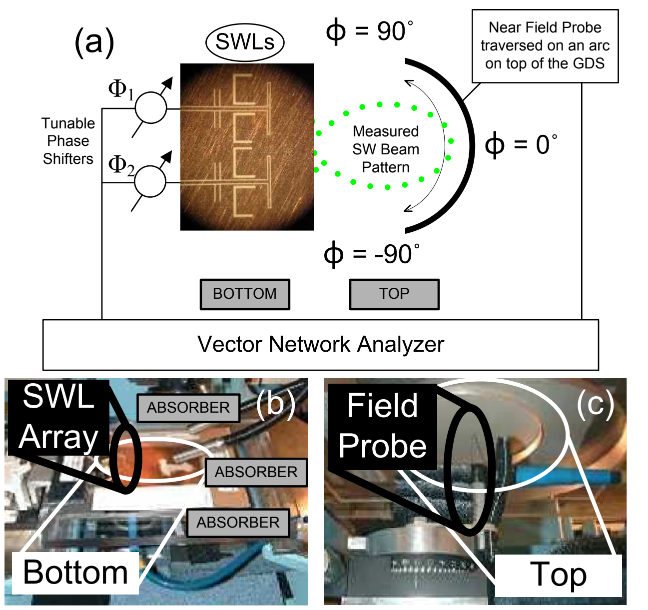

Fig. 6. Surface-wave beam pattern measurement system. (a): A near field probe (top) was used to measure the SW field distribution along the guiding surface. (b): The SWLs were excited on the bottom. (c): Probe mount.

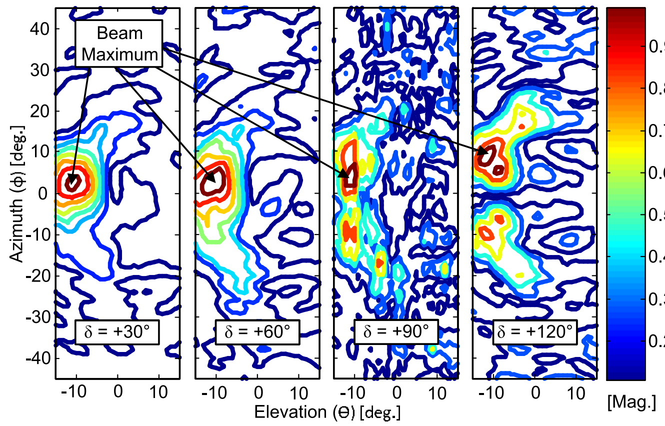

Fig. 8. Measured far field beam patterns at 19.2 GHz (normalized to observed maximum gain, shown in linear units) for $\delta = +30°, +60°, +90°$ and $+120°$. Minimal beam steering is observed. Similar results are expected for a negated relative phase difference.

The investigated metallic circular gratings (Fig. 1) can be defined by the radius of the m-th concentric ring, $\rho(m) = \rho_0 + p_\rho(m-1)$, where $\rho_0 = 10$ mm and $p_\rho = 6$ mm and the thickness of the strips is 1.25 mm for the fabricated design. Measured 2-D far field beam patterns are shown in Fig. 7 illustrating beam scanning as a function of frequency for $\delta = 0°$. In addition, by changing the relative phase difference between SWLs elements ($\delta = \pm 30°$, $\pm 60°$ and $\pm 90°$) conical-sector beam steering is observed (Figs. 8 - 12).

A. Measured Results and Theoretical Considerations

The inherent frequency dependent beam scanning is shown in Fig. 7. A broadside null is shown at 20.5 GHz suggesting a LW stopband and bound SW propagation along the guiding surface. In the backward region, at 19.2 GHz [19.5 GHz] the far field components are focused (as further discussed in [5]) generating a confined pencil beam and thus the far field steering capability is minimized as shown in Fig. 8 [Fig. 9]; specifically, for $\delta = +[-]30°, +[-]60°$, the main beam is located at $\theta = -11°$ $[-9°]$ and $\phi = -2°$ $[-2.5°]$ at 19.2 GHz [19.5 GHz]. Furthermore, for $\delta = +[-]90°, +[-]120°$ high SW side lobes are generated on the aperture realizing increased side lobe levels (with subsequently reduced gain in the main beams) in the far field. In general, similar results are expected for $\delta = -[+]30°$, $-[+]60°$, $-[+]90°$ and $-[+]120°$.

Conversely, conical-sector beam steering was observed for $21 \le f \le 23$ GHz (as shown in Figs. 7, 10 - 12) by tuning the relative phase difference between SWL sources. For instance, at 21.0 GHz the main conical-sector beam traces the path of a narrow cone from $\phi \in [+9°, -9°]$ at $\theta = 9°$ with an

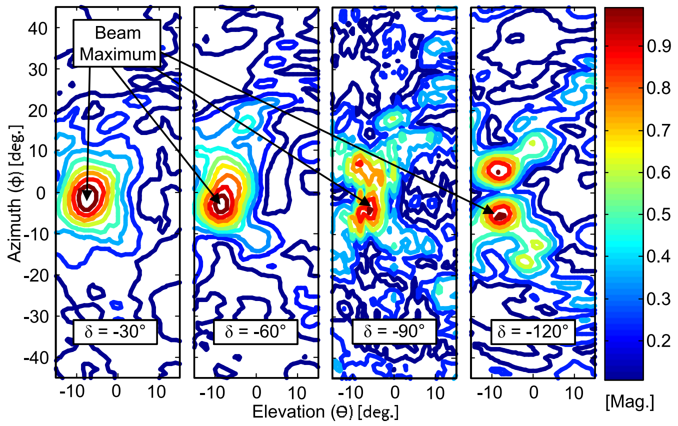

Fig. 9. Measured far field beam patterns at 19.5 GHz (normalized to observed maximum gain, shown in linear units) for $\delta = -30°, -60°, -90°$ and $-120°$. Minimal beam steering is observed. Similar results are expected for a negated relative phase difference.

element tuning range of $\delta = 0°, \pm30°, \pm60°$ and $\pm90°$. Minor beam steering is observed at this frequency since the generated pencil beam is very close to broadside. Furthermore, for $\delta = \pm90°$ a secondary beam is clearly observed at $\theta = +4°$ and $\phi = \pm10°$ due to increased SW side lobe levels.

As expected with this LWA, with an increase in frequency the main beam scans towards end fire and an improved steering range in the azimuth is possible as shown in Figs. 11 and 12. For instance, increased beam steering along a conical-sector, $\phi \in [0°, \pm10°]$ at $\theta = 12°$, is observed at 21.5 GHz. Furthermore, at 22.5 GHz the main beam is steered within a larger region, $\phi \in [0°, \pm13°]$ at $\theta = 26.5°$, in the far field.

B. Azimuth and Elevation Far Field Measurements

The 2-D far field beam patterns were obtained by measuring the investigated LWA in an anechoic chamber. The mechanical phase shifter was first calibrated for $\delta = 0°, \pm30°, \pm60°, \pm90°$ and $\pm120°$ at 19.2, 19.5, 20.5, 21.5 and 22.5 GHz. Then the LWA was translated in the azimuth and elevation (using a Newport ESP7000 Universal Motion Controller in 1° increments for $\theta \in [-15°, +35°]$ and $\phi \in [-45°, +45°]$) and measurements were conducted using a VNA (Anritsu 37377C) for each δ value and frequency point of interest. Results are shown in Figs. 7 - 12 with contour defining gain in the sampled azimuth and elevation planes.

IV. Conclusion

By varying the relative phase difference between a pair of SWLs bound SWs can be steered. Specifically, with a $\pm90°$ relative phase difference between SWL elements, a $\pm18°$ shift in the SW field distribution can be realized. Using such an antenna feeding network, measured 2-D beam patterns generated from a continuous circular strip grating LWA are presented for the first time. Results illustrate that the radiated pencil beam can be steered along a conical-sector from $\phi = +9°[+10°]\langle+13°\rangle$ to $\phi = -9°[-10°]\langle-13°\rangle$ at $\theta = 9°[12°]\langle26.5°\rangle$ in the far field at 21.0 [21.5] $\langle$22.5$\rangle$ GHz.

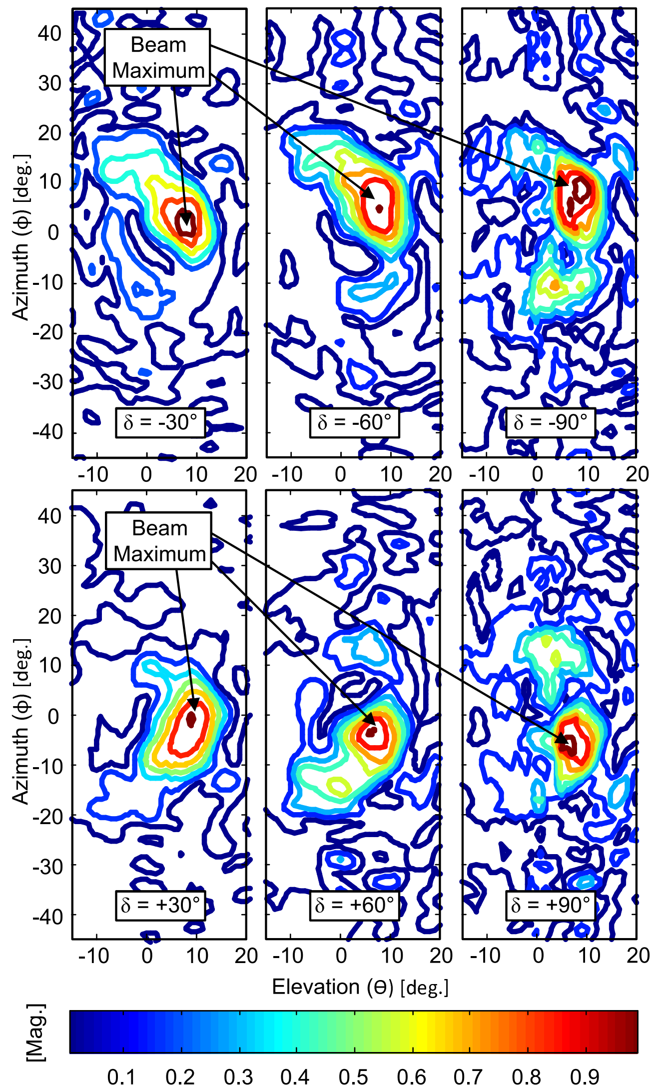

Fig. 10. Measured far field beam patterns at 21.0 GHz (normalized to maximum gain, shown in linear units) for $\delta = \pm30°, \pm60°$ and $\pm90°$. Beam steering along a conical-sector ($\phi \in [0°, \pm9°]$ at $\theta = 12°$) is observed.

References

[1] A. Ip and D. R. Jackson, "Radiation From Cylindrical Leaky Waves," *EEE Trans. Ant. Prop.*, vol. 38, no. 4, pp. 482–488, Apr. 1990.

[2] S. Mahmoud, Y. Antar, H. Hammad, and A. Freundorfer, "Theoretical Considerations in the Optimization of Surface Waves on a Planar Structure," *IEEE Trans. Ant. Prop.*, vol. 52, no. 8, pp. 2057–2063, Apr. 2004.

[3] H. Hammad, Y. Antar, A. Freundorfer, and S. Mahmoud, "Uni-Planar CPW-fed Slot Launchers for Efficient TM0 Surface Wave Excitation," *IEEE Trans. Micro. Theory Tech.*, vol. 51, no. 4, pp. 1234–1240, Apr. 2003.

[4] M. Ettorre, S. Bruni, G. Gerini, A. Neto, N. Llombart, and S. Maci, "Sector PCS-EBG Antenna for Low-Cost High-Directivity Applications," *IEEE Antennas and Wireless Propag. Lett.*, vol. 6, pp. 537-539, 2007.

[5] S.K. Podilchak, A.P. Freundorfer and Y.M.M. Antar, "Planar Leaky-Wave Antenna Designs Offering Conical-Sector Beam Scanning and Broadside Radiation using Surface-Wave Launchers," *IEEE Antennas and Wireless Propag. Lett.*, vol. 7, pp. 155-158, 2008.

[6] S.K. Podilchak, A.P. Freundorfer and Y.M.M. Antar, "Surface-Wave Launchers for Beam Steering and Application to Planar Leaky-Wave Antennas," *IEEE Trans. Ant. Prop.*, Accepted Oct. 2008.

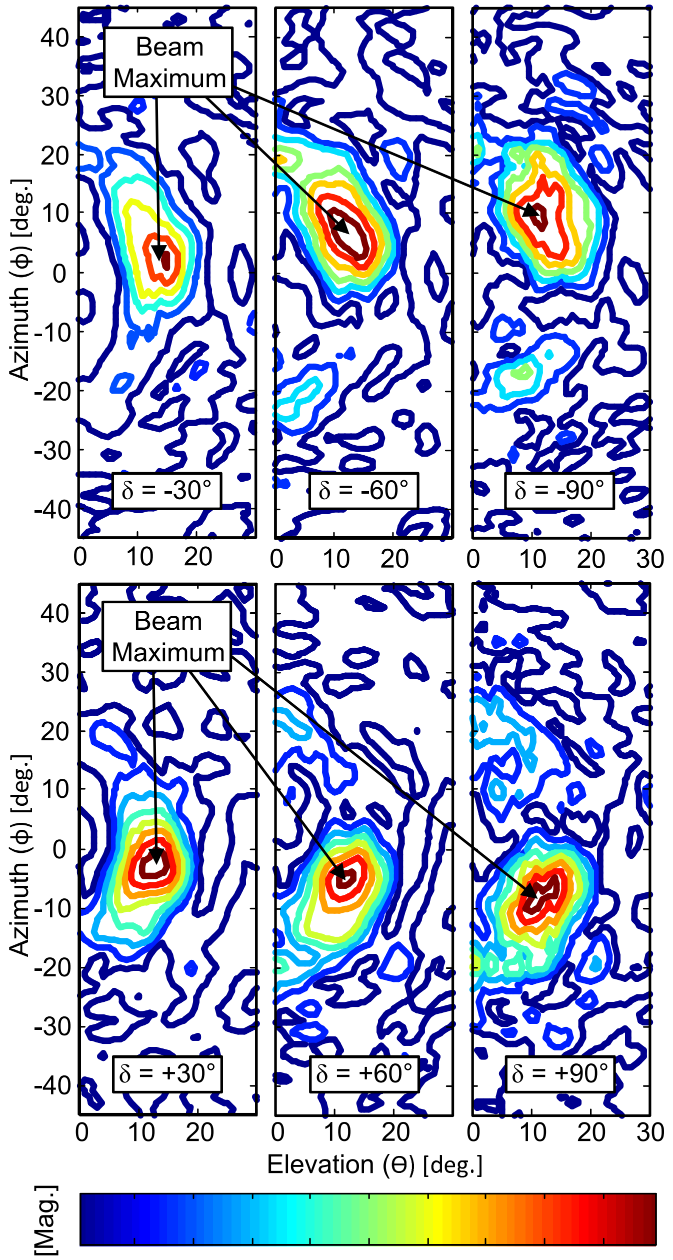

Fig. 11. Measured far field beam patterns at 21.5 GHz (normalized to maximum gain, shown in linear units) for $\delta = \pm 30°, \pm 60°$ and $\pm 90°$. Beam steering along a conical-sector ($\phi \in [0°, \pm 10°]$ at $\theta = 12°$) is observed.

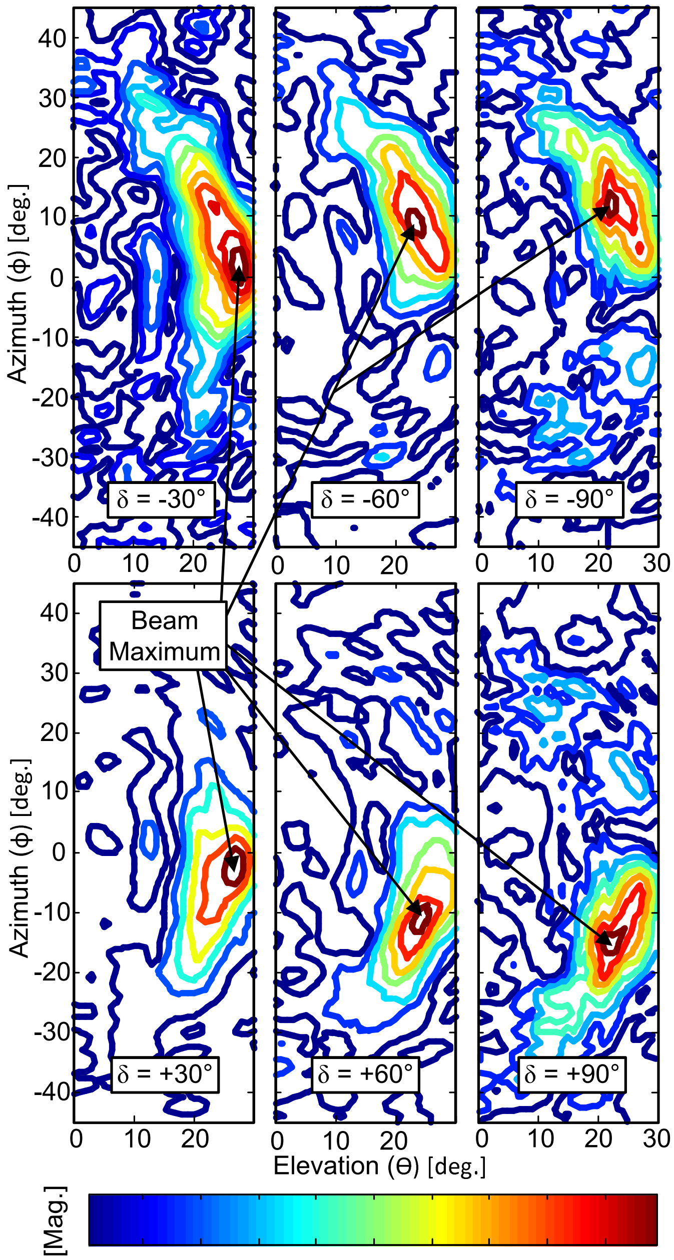

Fig. 12. Measured far field beam patterns at 22.5 GHz (normalized to maximum gain, shown in linear units) for $\delta = \pm 30°, \pm 60°$ and $\pm 90°$. Beam steering along a conical-sector ($\phi \in [0°, \pm 13°]$ at $\theta = 26.5°$) is observed.